Electrochemical Study of Oxygen Reduction Reaction on Natural Chalcopyrite in Sulfuric Acid and Ferric Solutions

Guobao Chen[*]*, Hong ying Yang*

School of Materials & Metallurgy, Northeastern University, Shenyang 110819, Liaoning, China
[*]E-mail: chengb@smm.neu.edu.cn

The oxygen reduction reaction (ORR) on the natural chalcopyrite electrode was investigated in sulfuric acid and ferric sulfate solutions, in terms of cyclic voltammetry (CV), linear sweep voltammetry (LSV) and rotating disc electrode (RDE). The tafel slopes and electron transferred numbers were also calculated. The ORR process took place in the potential range of -0.450 V to 0.050 V vs. AgCl/Ag. The average transferred electron number for ORR on chalcopyrite in sulfuric acid was near to 4. The addition of ferric ion was shown to increase the dissolution rate of chalcopyrite, however, the transferred electron numbers for ORR experienced a slight reduce and then grown fast with the increase of ferric ions. The ORR process was found to be inhibited attributing to a Fenton-like reaction mechanism at high concentration of ferric ions and more intermediate H_2O_2 was supposed to produce accordingly.
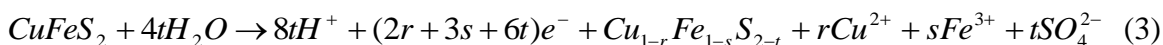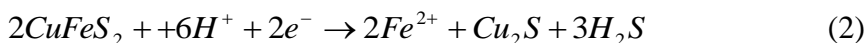
1. INTRODUCTION

Chalcopyrite ($CuFeS_2$) is known to occur in almost all sulfide minerals, but to be refractory in hydrometallurgical processes. Its leaching rate can be very low and reducing over time when the temperature is not very high [1, 2]. A number of studies have been reported to understand the leaching mechanisms and try to raise the recovery rate of copper from chalcopyrite. If the potential of the chalcopyrite increases during the dissolution process, the oxidation products on the surface will hinder the dissolution of chalcopyrite [3]. The formation mechanisms of these surface layers and their influences on the dissolution reaction are still in some dispute.

Several characterization methods, such as X-ray absorption (XAS), X-ray diffraction (XRD), synchrotron radiation X-ray photoelectron spectroscopy (SRXPS), auger electron spectroscopy (AES)

and optical microreflectometry (OMR), have been applied to examine the oxidized chalcopyrite [4]. Sulfur (S^0), disulfide (S_2^{2-}), metal deficient sulfide (S_n^{2-}) and ironic hydroxide formed on chalcopyrite surfaces during leaching in different media, have been all regarded as the causes of the passivation layer and various leaching mechanisms have been proposed according to these products [5-7]. However, Harmer et al. [8] found that when the special leaching conditions are applied, there will be no passivation. Some possible oxidation reactions for chalcopyrite dissolution in air have been proposed. These reactions include [4, 9-11]:

$$CuFeS_2 + 3H_2O \rightarrow Fe(OH)_3 + CuS + S^0 + 3H^+ + 3e^- \qquad (1)$$

$$2CuFeS_2 + + 6H^+ + 2e^- \rightarrow 2Fe^{2+} + Cu_2S + 3H_2S \qquad (2)$$

$$CuFeS_2 + 4tH_2O \rightarrow 8tH^+ + (2r + 3s + 6t)e^- + Cu_{1-r}Fe_{1-s}S_{2-t} + rCu^{2+} + sFe^{3+} + tSO_4^{2-} \quad (3)$$

There are two main oxidants of sulfides in sulfuric acid, the dissolved molecular oxygen and ferric ions. And most of the proposed leaching mechanisms are base on them. The previous reports majored in understanding the mechanisms and kinetics of chalcopyrite itself oxidative or reduction processes [12], while few studies are related to the reduction reactions of oxidants in the leaching systems. In fact, the reduction processes of oxidants will affect the whole leaching rate of chalcopyrite a lot and they should not be neglected. Before the overall mechanism of chalcopyrite dissolution are proposed accurately, several primary processes need to be understood such as: How does the nature of oxidants affect the surface products formed? [4] How does one oxidant affect the oxidation reactions of other oxidants? Nevertheless, the dissolved oxygen reduction behavior during chalcopyrite leaching process has been hardly conducted, and very few article studied the effects of ferric ions on the reduction processes of oxygen in leaching systems.

Thus the purpose of this study is to investigate the nature of oxygen reduction reactions on natural chalcopyrite surface in sulfuric acid. Besides, the effect of ferric ions on the ORR has also been evaluated. It is well known that in an oxidative sulfuric acid solution, chalcopyrite dissolution is essentially considered as an electrochemical corrosion process. So the electrochemical techniques are very useful tools to study the mechanism of ORR involved in the leaching process. A rotating disc electrode using natural chalcopyrite was prepared. Cyclic voltammetry, linear sweep voltammetry and rotating disc electrode methods had been applied to study ORR process. The tafel slope and the electron transfer number have been calculated according to the electrochemical test results.

2. MATERIALS AND METHODS

2.1 Mineral Electrode materials

A natural polycrystalline sample of chalcopyrite from Dabaoshan sulfur-polymetallic mines of China was used as electrode material. The chemical composition is analyzed by X-ray fluorescence (XRF). As shown in Figure 1, the purity of chalcopyrite sample is 96.51 %, and SiO_2 (3.32%) is the main impurity. The crystallinity of powder was characterized via X-ray diffraction (XRD). All the peaks appeared in the XRD spectrum are indexed to the phase of chalcopyrite ($CuFeS_2$). It can also be learned that there are no other phases of impurities, such as FeS or Cu_2S from this XRD pattern.
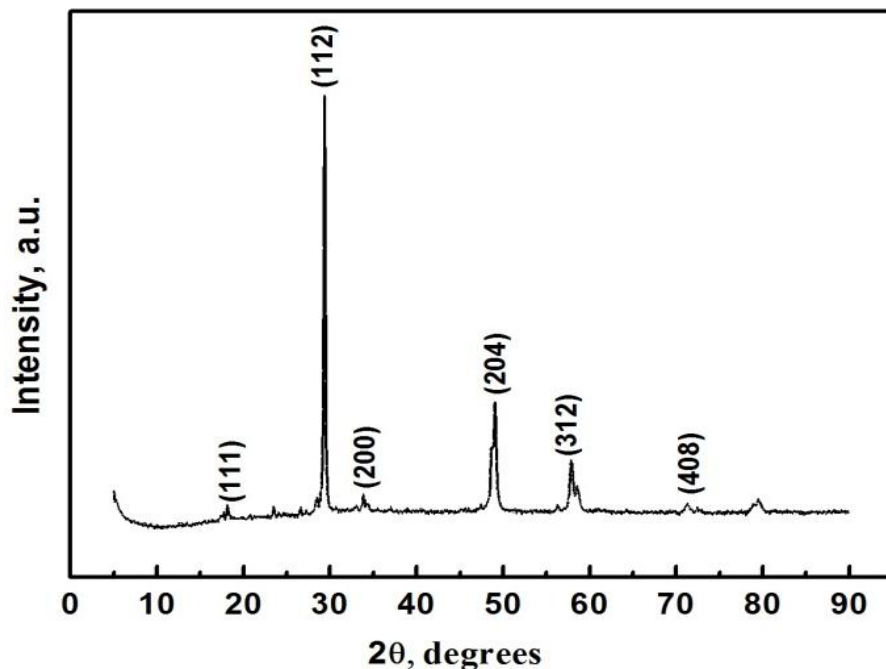
Figure 1. XRD spectrum of the $CuFeS_2$ natural sample

2.2 Rotating disk electrode preparation

Firstly, the massive chalcopyrite sample was cut into cylinders by a diamond wafering blade. The exposed area of obtaining specimens was controlled at 0.2374 cm^2, and its thickness was 1 cm. The cylinder samples were washed with double-distilled water firstly and then dried with analytical grade acetone. After that, a conducting silver paint (Dotite®, D-550) was applied to bond each specimen to a rotating copper bar. Then the prepared samples were sealed by Epoxy resin (Epofix®, Struers). These fresh electrodes were all experienced a wet mechanical polishing using SiC papers in the order of grit sizes 600, 1000 and 1200. The quality of the polished chalcopyrite surface was inspected via an optical microscope, and the morphology of the electrode need to remain similar to that observed before the previous experiment. The electrodes were then washed with de-ionized (DI) water and dried in a stream of compressed air.

2.3 Electrolyte solution preparation

Sulfuric acid (H_2SO_4, Fisher Scientific, dissolving reagent grade), and ferric sulfate pentahydrate ($Fe_2(SO_4)_3 \cdot 5H_2O$, 97%, Fisher Scientific) were used to prepare the solution with DI water. The sulfuric acid concentration of the solutions was always 0.5 M (pH = 0.3) and the addition of ferric ion in solution were 0, 0.05, 0.10, 0.50 and 10 g/L, respectively.

2.4 Electrochemical measurements

The nitrogen and oxygen concentration in the solution for all electrochemical experiments was controlled by sparging absolute gases through the solution. The solution volume was all 1000 mL of

fresh electrolyte. Each electrochemical experiment was conducted with a potentiostat/galvanostat 273A (Princeton Applied Research) controlled by Powersuite software. All electrochemical analysis was performed in a conventional three-electrode electrolytic cell. The test temperature of the cell was kept at a constant temperature 25 °C. The prepared chalcopyrite electrode was always used as the working electrode. A platinum wire (99.999%, Alfa Aesar) was served as a counter electrode, and the reference electrode was a Ag/AgCl/KCl (3.0 mol/L) reference electrode. A Luggin capillary was attached to the reference electrode to minimize the effect of the IR drop.

Before the start of all electrochemical tests, the ultra-pure gases (nitrogen or oxygen gas, 99.999%) were bubbled into the electrolyte solution for at least 20 min. The electrochemical measurements applied in the research include CV, LSV and RDE. By CV and LSV, the polarization current measurements of freshly prepared chalcopyrite electrodes were tested from 1.0 to -0.6 V vs. AgCl/Ag and from 1.0 to -0.5 V vs. AgCl/Ag, respectively. The scan rates were 20 mV/s and 2 mV/s respectively. For the RDE tests, the potential was scanned (2 mV/s) between 0.5 V and -0.5 V vs. AgCl/Ag with rotating rate ω = 100 - 2500 rpm. Before sweeping, the polished electrodes were immersed in the electrolyte for at least 20 min to obtain reproducible results.

3. RESULTS AND DISCUSSION

3.1 Cyclic voltammetry measurements
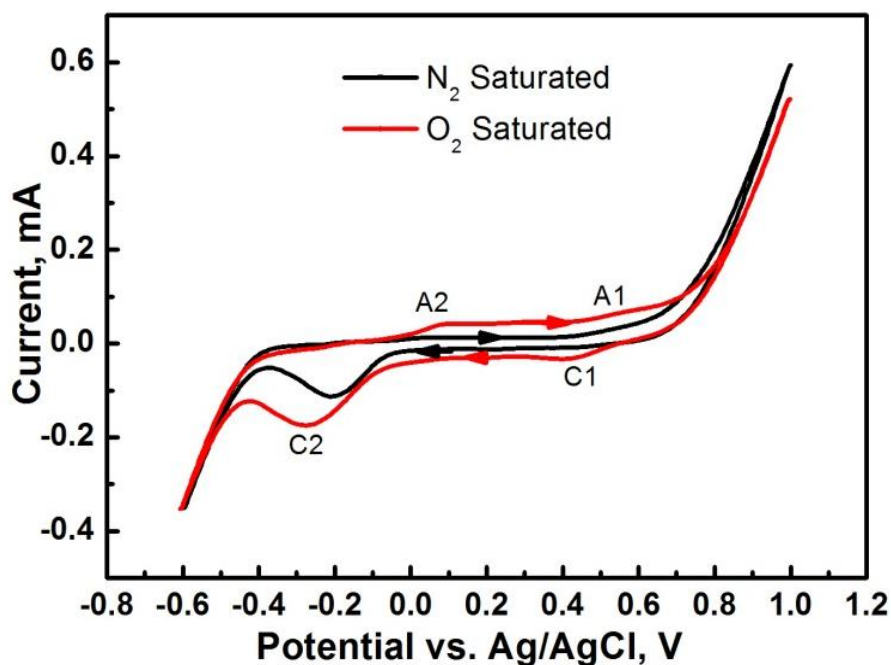
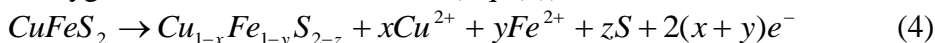
Figure 2. Cyclic voltammogramsrecorded at the chalcopyrite electrode in 0.5 M H_2SO_4 saturated with N_2 and O_2 respectively at 25 ℃. Potential scan rate: 20 mV/s.

Since the reactivity changes of chalcopyrite mineral are associated with its physical and chemical properties, firstly a wide potential window was carried out to determine the electrochemical behavior of the natural chalcopyrite.

For the cyclic voltammetry study, the scan started from the open circuit potential (OCP), the scan rate was 20 mV/s and the experiments were performed without stirring the electrolyte. The e electrochemical potential window was -0.600 V $\leqq E \leqq$ 1.00 V vs. AgCl/Ag.

Figure 2 shows the recorded at chalcopyrite disk electrodes in N_2 and O_2 saturated 0.5 M H_2SO_4 solutions respectively at 25 ℃. After reaching steady state for 30s, the OCP were measured to be 0.311 V and 0.348 V vs. AgCl/Ag for N_2 -saturated and O_2-saturated solutions respectively. For the O_2-saturated solution, two visible anodic peaks (A1 and A2) and two cathodic peaks (C1 and C2) were detected in the scan voltammogram, occurring in the potential range of $0.450 \leqq E_{A1} \leqq 0.650$ V, -0.100 V $\leqq E_{A2} \leqq 0.150$ V, 0.250 V $\leqq E_{C1} \leqq 0.550$ V, -0.450 V $\leqq E_{C2} \leqq 0.050$ V (vs. AgCl/Ag). For the N_2 -saturated solution, the peaks A1, A2 and C1 were not apparent and the peak currents were much lower than those in O_2 -saturated solution. The cathodic peak C1 probably corresponded to the reduction of chemical species formed during the positive-going scan [9]. Previous reports have proposed that under the steady-state condition (such as low redox potential values), the dissolution process of chalcopyrite combined simultaneously an anodic oxidation (Eq. (4)) with the reduction reaction of residual dissolved oxygen on the electrode surface (Eq. (5)) [13].

$$CuFeS_2 \rightarrow Cu_{1-x}Fe_{1-y}S_{2-z} + xCu^{2+} + yFe^{2+} + zS + 2(x+y)e^- \qquad (4)$$

$$4H^+ + O_2 + 4e^- \rightarrow 2H_2O \qquad (5)$$

Some researchers have believed that during the dissolution process in acidic media, the surface of chalcopyrite can form some intermediate products at low redox potentials (0.35-0.75 V vs. SHE). In generally, these intermediate products were metal-deficient sulfides, especially iron-deficient phases [10, 13].
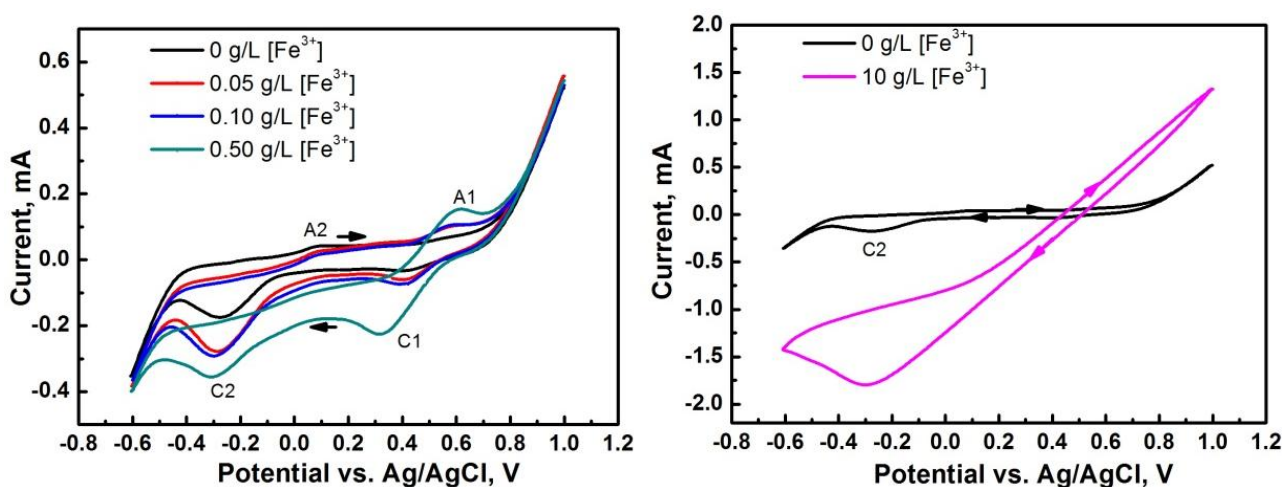

Figure 3. Cyclic voltammogramsrecorded at the chalcopyrite electrode in O_2 -saturated 0.5 M H_2SO_4 in the presence of ferric ions (the addition of ferric ions were 0, 0.05, 0.10, 0.50 and 10 g/L respectively) at 25 ℃. Potential scan rate: 20 mV/s.

Thus the peak C1 could be referred to the reduction of ferric according to the dissolution products of chalcopyrite (Eq. (4)). The intermediate phases formed on mineral surface are commonly considered to inhibit the reaction progress, which named as "passivation". This may be the reason that the peak current of C1 is very low. It is worth noting that the peak current of C2 in O_2 -saturated solution is about twice as that in N_2 -saturated solution. Considering there is no other significant oxygen-dependent reaction except the oxygen reduction reaction (ORR) (Eq. (5)), the cathodic peak C2 can be inferred as the ORR result. And the anodic processes A1 and A2 can be attributed to the oxidation of chalcopyrite and the activation of water respectively.

Figure 3 presents the cyclic voltammograms traced on the chalcopyrite sample in O_2 -saturated 0.5 M H_2SO_4 in the presence of ferric ions at 25 ℃. The concentration of ferric ions varied from 0 to 10 g/L. Four peaks were also identified as A1, A2, C1 and C2. The potential ranges were similar to those in Fig. 2, while the peak currents changed a lot with different concentration of ferric ions in the solution. On comparing the voltammograms, C1/A1 processes were distinguishable and became increasingly better defined as the addition of ferric ions increasing from 0 to 0.50 g/L. Peaks C1 and A1 were separated by 140 mV when the concentration of ferric ions were below 0.50 g/L. It turned to nearly 300 mV with the ferric ions was controlled at 0.50 g/L. This maybe due to that the processes were not only associated with the reduction-oxidation of the chalcopyrite (Eq. (4)), but also involved in the ferric ion reduction and ferrous oxidation in the solution (Eq. (6)).

$$Fe^{3+} + e^- \rightarrow Fe^{2+} \qquad\qquad (6)$$

It is interesting to find that there was no visible C1/A1 peaks when the content of ferric ions was 10 g/L. In high concentration of ferric ions, the main reaction for the chalcopyrite electrode is ferric sulfate leaching reaction of chalcopyrite, according to the reaction as follows [14].

$$CuFeS_2 + 4Fe^{3+} \rightarrow Cu^{2+} + 5Fe^{2+} + 2S \qquad\qquad (7)$$
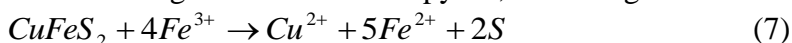
As discussed above, the peaks C2 and A2 were corresponding to ORR and water oxidation reaction respectively. With the increase of ferric ions, the peak current of C1 increased while that of A1 reduced obviously. Both the potential ranges of C2 and A2 were seemed more stable with the increase of ferric ions. Thus it can be inferred that the ferric content can influence the reaction dynamics oxygen-dependent reaction.

3.2 Linear sweep voltammetry measurements

The polarization curve measurements were performed at a rate of 2 mV/s, from -0.500 V to 1.00 V vs. AgCl/Ag. After a 20 min immersion in the electrolyte, the experimental data were recorded and the electrode rotating speed was controlled at 400 rpm.

Figure 4 exhibits the tafel plots for chalcopyrite in N_2 and O_2 saturated 0.5 M H_2SO_4 respectively (Fig. 4a) and in O_2 -saturated 0.5 M H_2SO_4 with the presence of ferric ions (the addition of ferric ions were 0, 0.05, 0.10, 0.50 and 10 g/L respectively) at 25 ℃ (Fig. 4b). As shown in Fig. 4a, the tafel slopes $b = \dfrac{\partial E}{\partial \log i}$ in cathodic branch were calculated and they were 0.305 and 0.314 V decade^{-1} for the O_2-saturated and N_2-saturated solution respectively. The more notable difference for the two

solutions was the corrosion potentials, which were 0.538 V and 0.310 V vs. AgCl/Ag, proving that oxygen plays an important oxidation role for dissolution of chalcopyrite, as discussed above (Eq. (5)).
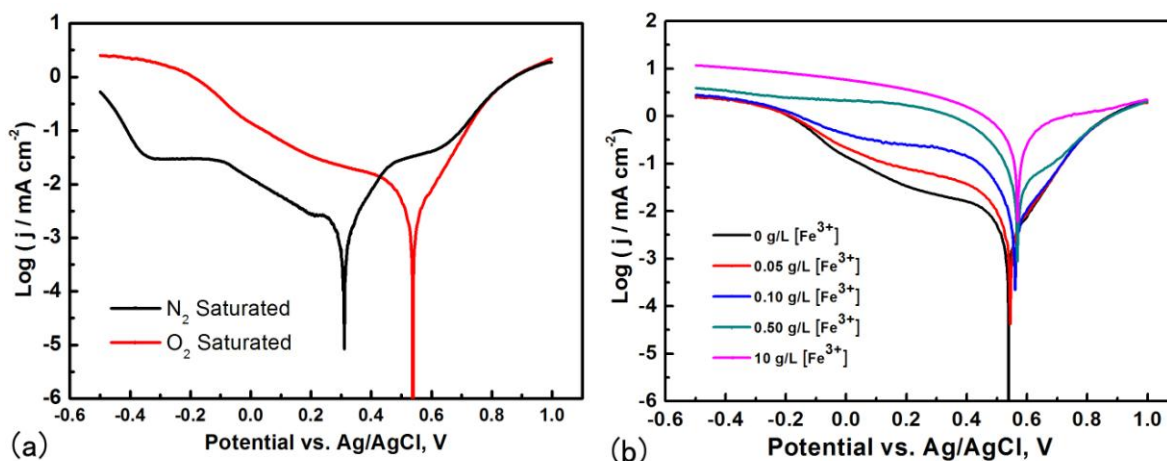
Figure 4. (a) Tafel plots for chalcopyrite in 0.5 M H_2SO_4 saturated with N_2 and O_2 respectively at 25 ℃; (b) Tafel plots for chalcopyrite in O_2-saturated 0.5 M H_2SO_4 with the presence of ferric ions (the addition of ferric ions were 0, 0.05, 0.10, 0.50 and 10 g/L respectively) at 25 ℃. Potential scan rate: 2 mV/s; rotation speed: 400 rpm.

From Fig. 4b, it can be noted that the current increase with the addition of ferric ions when the potentials below 0.500 V vs. AgCl/Ag. The observed increasing current could be associated with the reduction rates of the two oxidants, oxygen and ferric ions, on the solid surface [10]. It can also be calculated that with the ferric ion concentration came to 0, 0.05, 0.10, 0.50 and 10 g/L, the tafel slopes in cathodic branch were 0.305, 0.326, 0.373, 1.34 and 1.77 V/decade, respectively. This suggests that the ORR process on the natural chalcopyrite becomes more difficult with the addition of ferric ions. Despite this, the corrosion potentials are not changed a lot from the Fig. 4b, less than 40 mV after ferric ions were added. This may be due to the weakened ORR kinetics, though the ferric ion can enhance the dissolution speed of chalcopyrite.

3.3 Rotating disk electrode measurements

It is well known that there are two main routes for the ORR process in an acidic media [15]: one is the production of water through the direct four-electron reduction reaction (Eq. (8)); the other one is the production of hydrogen peroxide though the two-electron reduction reaction (Eq. (9)), which can be finally reduced to water through reaction (Eq. (10)).

$$4H^+ + O_2 + 4e^- \rightarrow 2H_2O \qquad E_0 = 1.229 \text{ V vs.NHE} \qquad (8)$$

$$2H^+ + O_2 + 2e^- \rightarrow 2H_2O_2 \qquad E_0 = 0.67 \text{ V vs.NHE} \qquad (9)$$

$$2H^+ + H_2O_2 + 2e^- \rightarrow 2H_2O \qquad E_0 = 1.77 \text{ V vs.NHE} \qquad (10)$$

In order to confirm the mechanism of oxygen reduction on natural chalcopyrite further, the numbers of electrons transferred per O2 molecule were also calculated with the following Koutecky– Levich equation [16].
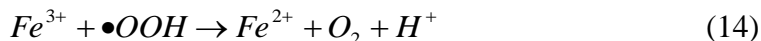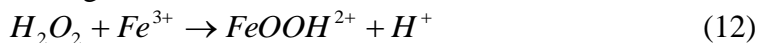
$$-\frac{1}{J} = \frac{1}{J_k} + \frac{1}{0.62nFAD^{2/3}cv^{-1/6}\omega^{1/2}} \tag{11}$$

where J_k is the kinetic current; n is the number of exchanged electrons per reduced oxygen molecule involved in the whole reaction; F is Faraday constant (96,485 C mol^{-1}); A is thegeometric area of the disk electrode (0.2374 cm^{-2}); D is the diffusion coefficient of the dissolved oxygen in electrolyte (1.93 × 10^{-5} cm^2 s^{-1}); c is the concentration of dissolved oxygen in 0.5 M H$_2$SO$_4$ (1.13 × 10^{-6}mol cm^{-3}); v is the kinematic viscosity of the electrolyte (9.5 × 10^{-3} cm^2 s^{-1}) ; ω is the rotation rate [17].
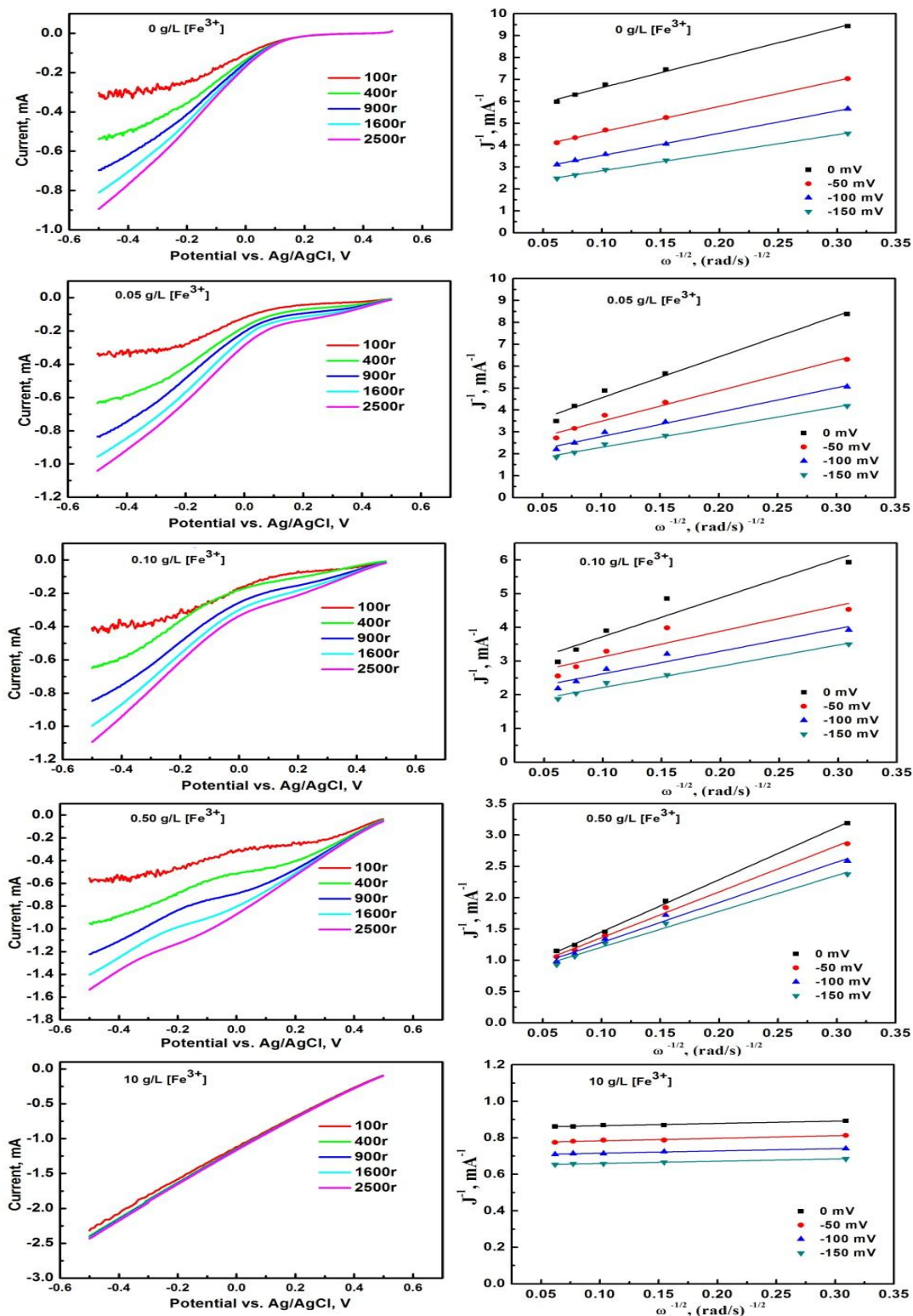
Figure 5 shows the RDE measurement results for oxygen reduction reaction on chalcopyrite in 0.5 M O$_2$ -saturated H$_2$SO$_4$ in the presence of ferric ions (the addition of ferric ions were 0, 0.05, 0.10 and 0.50 g/L respectively) and corresponding Koutecky-Levitch (K-L) (J^{-1} versus ω$^{-1/2}$) plots. The rotating speeds were set at 100, 400, 900, 1600 and 2500 rpm respectively. It is observed that the J^{-1} and ω$^{-1/2}$ have a good linear relationship at different electrode potentials. However, the plots have not exhibited a good parallelism after the ferric ions were added, indicating that the ORR mechanism was changed by the addition of ferric ions, and an incomplete reduction of oxygen to water may occur at some potentials.

Based on the K-L plots, the electron transfer number of the ORR obtained according to Eq. (11), and the dependence of n on potential for chalcopyrite were summarized and shown in Figure 7. It is obviously that when the concentration of ferric ions below 10 g/L, the n values reduced with the increase of potentials from -150 to 0 mV vs. AgCl/Ag. This is due to the fact that at high overpotential (-150 mV vs. AgCl/Ag) the driven force for the reductive reaction is greater, and more intermediates are reduced in comparison with that at low overpotential (0 mV vs. AgCl/Ag). It can be calculated that the average number for ORR in sulfuric acid is 3.77, near to 4, suggesting that it was a direct four-electron reduction through reaction (Eq. (8)). With the increase of ferric concentration from 0 to 0.50 g/L, the transferred electron number varies from about 7 to 2, indicating that the ORR pathway is dependent on the media concentration.

It has been proposed that the whole reduction process of oxygen is 2-electron reduction combined 4-electron reduction. In dilute solutions, after molecular oxygen direct chemisorbed on a chalcopyrite site, the ORR pathway will undergo the inner-sphere electron transfer mechanism, and cause to a direct or a series 4e pathway without the desorption of reaction intermediates (i.e., peroxide) from the mineral surface according to reactions (Eq. (8-10)). However, the peroxide intermediate is not stable at these potentials and when the ferric ions were added, the formed peroxide may be reduced further by ferrous ions in the solution according to the reaction (Eq. (6)). This may be the reason why the n value is lower after 0.05 g/L ferric ions were added in the solution. However, when the ferric ions continue rising, Fe^{3+} can react with H$_2$O$_2$ in the so-called Fenton-like reaction [18, 19]:

$$H_2O_2 + Fe^{3+} \rightarrow FeOOH^{2+} + H^+ \tag{12}$$

$$FeOOH^{2+} \rightarrow Fe^{3+} + \bullet OH \tag{13}$$

$$Fe^{3+} + \bullet OOH \rightarrow Fe^{2+} + O_2 + H^+ \tag{14}$$

Figure 5. Rotating disk electrode measurements for oxygen reduction reaction on chalcopyrite in O_2 - saturated 0.5 M H_2SO_4 in the presence of ferric ions (the addition of ferric ions were 0, 0.05, 0.10, 0.50 and 10 g/L respectively) at 25 ℃ (Left figures); Corresponding Koutecky-Levich plots at different potentials: 0 mV, -50 mV, -100 mV and -150 mV obtained the data from left figures respectively (Right figures). Disk area: 0.2374 cm^2; potential scan rate: 2 mV/s.

The RDE results in Fig. 6 shows that the Fenton-like reaction maybe refer to a multi-electron transfer process, and the transferred electron numbers increased apparently when the addition of ferric ions increases from 0.05 g/L to 10 g/L. Though the Fenton-like reaction can lead to a very fast reaction [19], the efficient usage of oxygen for ORR is quite low since the O_2 reproduction in the reaction (Eq. (14)). It can be also proved by the Fig. 5 that there is almost no ORR peak for the polarization curves when the ferric ions concentration came to 10 g/L.

The proposed mechanism is in agreement with other researches where it was reported that with an increase in pyrite proportion of mineral, the chalcopyrite dissolution enhanced [20] and the content of H_2O_2 increased [21]. The formation of higher quantity of hydrogen peroxide with the presence of ferric ions in the electrolyte may explain not only the effects of interaction between the minerals and iron containing electrolyte, but also the influence of pyrite on other sulphide minerals in the context of leaching, froth flotation, geochemical processes and environmental controls. While until now, most literature has assumed as galvanic interactions and electron transfer from one to others [4, 20, 22-24].

The formation of hydroxyl radical was supported by experimental test data in the previous reports [21, 25, 26]. E_h-pH stability diagram of chalcopyrite was also used to discuss the formation of ferric oxide or hydroxide at high E_h value in acidic conditions, and ferric ions were found to generate H_2O_2 [21]. The superoxide was supposed to form at acidic pH in the presence of dissolved oxygen molecular (Eq. (15, 16)).

$$O_2 + e^- \rightarrow (O_2^\bullet)^- \qquad (15)$$

$$2(O_2^\bullet)^- + 2H^+ \rightarrow H_2O_2 + O_2 \qquad (16)$$
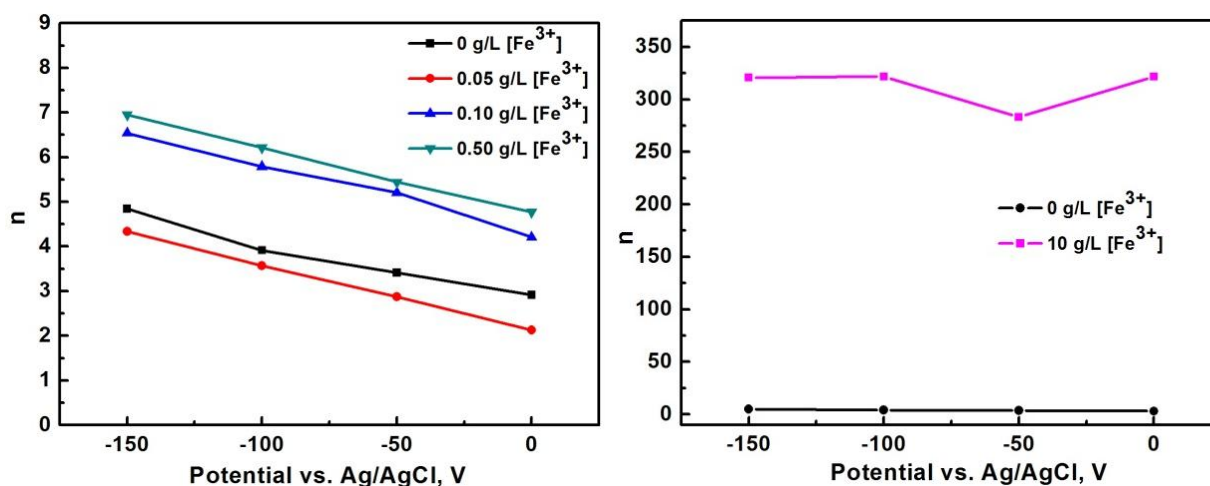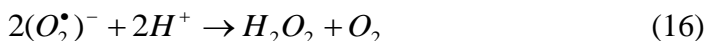
Figure 6. Effect of potential on the electron tranfer numbers for natural chalcopyrite in different ferric solutions.

4. CONCLUSIONS

In summary, the oxygen reduction reaction on the natural chalcopyrite electrode in sulfuric acid and ferric sulfate solutions were studied by cyclic voltammetry, linear sweep voltammetry and rotating disc electrode methods. The electron transferred numbers of ORR process were calculated and the

effect of ferric ion on ORR process was also quantified. The results showed that the ORR occurred on the chalcopyrite in the potential range of -0.450 V to 0.050 V vs. AgCl/Ag. The tafel slopes for the ORR processes increased from 0.305 to 1.34 V/decade with the addition of ferric ions. It was demonstrated that the transferred electron numbers reduced with the raising potential and the average number for ORR in sulfuric acid is near to 4. While after the ferric ions were added, the transferred electron numbers experienced a slight reduce when ferric ions concentration was 0.05 g/L, and then grow fast with the increase of ferric ions. The ORR process was considered to be inhibited by the large amounts of ferric ions according to the proposed Fenton-like reaction mechanism and more intermediate H_2O_2 was supposed to produce.

References

1. T. Hirato, H. Majima, and Y. Awakura, *Metall. Mater. Trans. B*, 18 (1987) 489.
2. C. Klauber, *Int. J. Miner. Process.*, 86 (2008) 1.
3. H. Zhao, J. Wang, W. Qin, M. Hu, S. Zhu, and G. Qiu, *Miner. Eng.*, 71 (2015) 159.
4. Y. Li, N. Kawashima, J. Li, A.P. Chandra, and A. Gerson, *Adv. Colloid Interface Sci.*, 197 (2013) 1.
5. H. Zhao, J. Wang, W. Qin, M. Hu, and G. Qiu, *Int. J. Electrochem. Sci.,* 10 (2015) 848.
6. C. Klauber, A. Parker, W.V. Bronswijk, and H. Watling, *Int. J. Miner. Process.*, 62 (2001) 65.
7. R.P. Hackl, D.B. Dreisinger, E. Peters, and J.A. King, *Hydrometallurgy*, 39 (1995) 25.
8. S.L. Harmer, J.E. Thomas, and D. Fornasiero, *Geochim. Cosmochim. Acta*, 70 (2006) 4392.
9. D. Nava and I. Gonz´alez, *Electrochim. Acta*, 51 (2006) 5295.
10. D. Majuste, V.S.T. Ciminelli, and K. Osseo-Asare, *Hydrometallurgy*, 111 (2012) 114.
11. A. Ghahremaninezhad, D.G. Dixon, and E. Asselin, *Electrochim. Acta*, 87 (2013) 97.
12. G. Yue and E. Asselin, *Electrochim. Acta*, 146 (2014) 307.
13. G. Parker, R. Woods, and G. Hope, *Colloids Surf. A*, 318 (2008) 160.
14. P.B. Munoz, J.D. Miller, and M.E. Wadsworth, *Metall. Mater. Trans. B*, 10 (1979) 149.
15. E. Yeager, *Electrochim. Acta*, 29 (1984) 1527.
16. S. Ye and A. K. Vijh, *J. Solid State Electrochem.*, 9 (2005) 146.
17. M.S. El-Deab and T. Ohsaka, *Electrochim. Acta*, 47 (2002) 4255.
18. E. Brillas, I. Sire´s, and M.A. Oturan, *Chem. Rev.*, 109 (2009) 6570.
19. M.C. Pereira, L.C.A. Oliveira, and E. Murad, *Clay Miner.,* 47 (2012) 285.
20. O.G. Olvera, L. Quiroz, D.G. Dixon, and E. Asselin, *Electrochim. Acta*, 127 (2014) 7.
21. A. Nooshabadi, and K. Rao, *Hydrometallurgy*, 141 (2014) 82.
22. A. Akcil, and H. Ciftci, *Int. J. Miner. Process.*, 71 (2003) 233.
23. C. Owusu, D. Fornasiero, J. Addai-Mensah and M. Zanin, *Int. J. Miner. Process.*, 134 (2015) 50.
24. G. Huang, and S. Grano, *Miner. Eng.*, 18 (2005) 1152.
25. A. Nooshabadi, and K. Rao, *Miner. Metall. Process.*, 30 (2013) 212.
26. G. Jones, M. Becker, R. Hille, and S. Harrison, *Appl. Geochem.*, 29 (2013) 199.